ISSN 1070-3284, Russian Journal of Coordination Chemistry, 2024, Vol. 50, No. 5, pp. 326–333. © Pleiades Publishing, Ltd., 2024.

Interaction of Lyophilic Zinc(II) Porphyrins with Bovine Serum Albumin

O. I. Koifman[a, b, †], N. Sh. Lebedeva[a], E. S. Yurina[a, *], Yu. A. Gubarev[a], S. A. Syrbu[a, b], A. N. Kiselev[a], and M. A. Lebedev[a, b]

[a] *Krestov Institute of Solution Chemistry, Russian Academy of Sciences, Ivanovo, Russia*

[b] *Ivanovo State University of Chemistry and Technology, Ivanovo, Russia*

**e-mail: yurina_elena77@mail.ru*

Received December 20, 2023; revised February 6, 2024; accepted February 16, 2024

Abstract—Palladium-catalyzed heterylation of monobromophenyl-substituted zinc(II) porphyrin with small heterocycles (benzothiazole, benzoxazole, and N-methylbenzimidazole) was carried out. As a result, unsymmetrical heterylphenyl-substituted zinc(II) porphyrins soluble in organic solvents were obtained. The interaction of heteryl-substituted zinc(II) porphyrins with alpha-helical proteins was studied by spectral methods using bovine serum albumin in aqueous organic solvents. It was found that the titration of the zinc(II) porphyrins with albumin in a sodium phosphate buffer involves a number of equilibria including complexation and aggregation. In the case of porphyrins containing N-methylbenzimidazole and benzoxazole residues, self-aggregation processes initiated by absorption of organic solvent molecules by the protein predominate. It was found that more hydrophobic nature of zinc(II) porphyrin with benzothiazole residue promotes the complex formation with the protein. The photochemical properties of zinc(II) porphyrin with a benzothiazole residue, capacity for the photooxidation of the alpha-helical protein, and the high affinity of protein to this porphyrin make it a promising candidate for the potential applicability for photodynamic inactivation.

Key words: zinc(II) porphyrins, heteryl-substituted porphyrins, synthesis, protein, complex, photoinactivation

DOI: 10.1134/S1070328424600244

INTRODUCTION

Microbial infections remain the leading cause of human mortality worldwide [1, 2]. The appearance of multidrug-resistant pathogenic bacteria is a major factor leading to infectious disease pandemic. In 2019, the World Health Organization (WHO) ranked antimicrobial resistance (AMR) as one of the top ten threats to global health [3]. Thus, the search for new, more efficient antibacterial treatment methods has become the subject of intensive and continuous research [4]. The use of photodynamic inactivation (PDI) as an antibiotic-free approach to inactivate pathogens seems very promising [5–7]. Porphyrins are the best photosensitizers for PDI, which is due to their unique photochemical properties and virtually unlimited options of their functionalization to increase the selectivity of binding to a particular target biosubstrate [8–10]. Previously, we obtained good results in the detection of lytic activity of Gram-positive staphylococcus bacteria by water-soluble unsymmetrically substituted porphyrins containing heterocyclic moieties at the periphery of the porphyrin core [11]. It is noteworthy that the preparation of water-soluble porphyrins is faced with a number of problems: laborious and multistep synthesis and difficult purification of the ready product. In this respect, it is more promising to use organosoluble porphyrins as potential photosensitizers for inactivation of bacteria and pathogens. One way for penetration of a photoinactivating agent into the cell is interaction with the alpha-helical transmembrane proteins, which have a high affinity to lyophobic compounds. Transmembrane proteins are integral proteins of a cell membrane; they are aggregated in aqueous media and are unstable to sedimentation. Therefore, the primary studies are performed using model alpha-helical proteins: albumins. The possibility of interaction of globular proteins with hydrophobic natural porphyrins was demonstrated earlier [12–16].

The purpose of the present work is to study the interaction of unsymmetrical synthetic porphyrins with alpha-helical proteins using bovine serum albumin as an example.

† Deceased.

EXPERIMENTAL

Bovine serum albumin (BSA), fraction V (Acros Organics) was used. All solutions were prepared in a PBS buffer (Sigma-Aldrich) with pH 7.4. Solutions were prepared using type I water (18 MΩ/cm) produced by the UP-2010 water treatment system, ULAB (China). The solubility of porphyrins was provided by using DMF (analytical grade). The solutions were prepared in such a way that the BSA concentration was 0.08 wt % and the DMF concentration did not exceed 0.19 M [19, 20]. The solvents were dried and distilled prior to use. Compounds of at least 99% purity were used (Reakhim, EKOS-1, Aldrich, Fluka).

The electronic absorption (UV-Vis) and fluorescence spectra of albumin and its complexes with porphyrins were recorded on an AvaSpec-2048 spectrophotometer (Avantes BV, the Netherlands) at 25°C in a temperature-controlled cell. A LEDUVTOP-295 monochromatic light-emitting diode (Sensor Electronic Technology, Inc., USA) was used as a source of excitation light to study albumin fluorescence.

The fluorescence lifetime was determined using a FluoTime 300 high-performance fluorescence lifetime and steady state fluorescence spectrometer (Pico Quant, Germany) with a 450 nm laser as the excitation source. The instrument response function (IRF) of the system was measured using the scattered light signal from a dilute suspension of colloidal silicon dioxide (LUDOX®). The fluorescence decay curves were measured and fluorescence lifetimes were found by deconvolution of the decay curves using the EasyTau 2 software package (PicoQuant, Germany).

The quantum yield of singlet oxygen was determined from the photolysis of 1,3-diphenylisobenzofuran [17] in air-saturated DMF using the equation $\Phi_\Delta = \Phi_\Delta^{Std} \frac{RI_{abs}^{Std}}{R^{Std} I_{abs}}$, where Φ_Δ^{Std} is the quantum yield of singlet oxygen generated by 5,10,15,20-tetraphenylporphyrin, which is 0.64 in DMF [18]. The R^{Std} and R values are the rates of photolysis of 1,3-diphenylisobenzofuran in the presence of standard and test compounds, respectively. The amount of light absorbed by the standard I_{abs}^{Std} and by the test compound I_{abs} was determined radiometrically using an AvaSpec-2048 spectrophotometer (Avantes BV).

The fluorescence quantum yield was determined using the ZnTPP standard by the procedure described previously [19].

The UV-Vis spectra of the test compounds were measured in dichloromethane on a UV/VIS Hitachi U2001 spectrophotometer (Japan) at room temperature in the 200–1000 nm range. ^{1}H NMR spectra were run on a Bruker Avance-500 instrument (USA). The solvent signals were used as internal standards. The positive-ion MALDI-TOF mass spectra were recorded on a Shimandzu AXIMA Confidence matrix-assisted laser desorption ionization time-of-flight mass spectrometer (Japan) and on a Bruker Daltonics Ultraflex instrument (USA). The identity and purity of compounds were established by TLC (Silufol).

Synthesis of 5(4'-bromophenyl)-10,15,20-triphenylporphin (Por). A solution of pyrrole (5 mL, 72 mmol), 4-bromobenzaldehyde (3.3 g, 18 mmol), and benzaldehyde (5.5 mL, 54 mmol) in *para*-xylene (50 mL) was added from a dropping funnel over a period of 20 min to a refluxing solution of trifluoroacetic acid (2 mL) in *para*-xylene (250 mL) in a flow of nitrogen. The mixture was refluxed for 40 min in a nitrogen flow and then for 1 h in an air flow. The solution was cooled and neutralized with a 25% ammonia solution (20 mL). Xylene was distilled off with steam, and the residue in the flask was collected on a filter, dried at room temperature, dissolved in chloroform (200 mL), and chromatographed on an Al_2O_3 column (Brockmann activity II), using a chloroform–hexane mixture (1 : 1) as the eluent. The first dark red band of 5-(4'-bromophenyl)-10,15,20-triphenylporphin containing tetraphenylporphin by-product as an impurity was collected. The eluate was evaporated to 5 mL, and monobromoporphyrin was precipitated with methanol (50 mL) and dried at room temperature to a constant weight. The yield was 1.14 g (23%). R_f 0.67 (Silufol, chloroform). UV-Vis (chloroform), λ_{max}, nm (logε): 648(3.63), 590(3.77), 551(3.91), 515(4.26), 491(5.64). MS (MALDI-TOF), *m/z*: was calculated for $C_{44}H_{29}N_4Br$ 693.6312; found, 694.4227 $[M + H]^+$.

Synthesis of zinc 5-(4'-bromophenyl)-10,15,20-triphenylporphin (ZnPor). Por (3 g, 4.3 mmol) and anhydrous zinc acetate (4.7 g, 0.021 mol) were dissolved in a mixture of methanol (200 mL) and chloroform (100 mL). The mixture was refluxed for 1.5 h; the course of the reaction was monitored by UV-Vis spectroscopy. The mixture was cooled, the excess solvent was evaporated, and the residue was chromatographed on a column with Al_2O_3 (Brockmann activity III), using chloroform as the eluent. The solvent was evaporated, and the residue was washed with water, collected on a filter, and dried at room temperature to a constant weight. The yield was 3.3 g (98%).

^{1}H NMR (δ, ppm): 9.02–8.99 (m, 2H, $H^{8,12}$), 8.97–8.96 (m, 2H, $H^{2,18}$), 8.27–8.24 (m, 4H, $H^{3,7,13,17}$), 8.14–8.12 (m, 1H, $H^{4\text{-HPh}}$), 7.78–7.73 (m, 10H; 8H, $H^{2,6\text{-HPh}}$; 2H, $H^{4\text{-HPh}}$), 7.59–7.51 (m, 8H, $H^{3,5\text{-HPh}}$) ($CDCl_3$). UV-Vis: λ_{max} (nm, logε): 595(3.70), 551(4.14), 424(5.51) ($CHCl_3$). MALDI-TOF MS, *m/z*: calculated for $C_{44}H_{27}N_4BrZn$ 757.0156; found: 757.5608.

Synthesis of zinc 5-[4'-(1",3"-benzothiazol-2"-yl)phenyl]-10,15,20-triphenylporphin (ZnPorS). In a 100-mL flask equipped with a magnetic stirrer and reflux condenser, a mixture of ZnPor (1 g, 0.132 mmol), $Pd(OAc)_2$ (0.0592 g, 0.264 mmol),

$Cu(OAc)_2 \cdot H_2O$ (0.0575 g, 0.264 mmol), triphenylphosphine (0.34 g, 0.132 mmol), potassium carbonate (0.364 g, 1.342 mmol), and benzothiazole (290 μL, 0.264 mmol) in toluene (45 mL) was refluxed with stirring for 52 h. Then the mixture was cooled to room temperature, dichloromethane (50 mL) was added, and the solution was filtered. The precipitate was washed with dichloromethane (10 mL), and the combined organic fractions were evaporated in vacuo. The residue was dissolved in dichloromethane (30 mL) and chromatographed on a silica gel column; elution was performed first with a hexane–dichloromethane mixture (1 : 1) (to collect the tetraphenylporphin impurity band) and then with dichloromethane to collect the dark red monoheterylporphyrin band. The solvent was evaporated to dryness. The yield was 0.152 g (75%). R_f 0.61 (Silufol, chloroform). ^{1}H NMR (δ, ppm): 8.99–8.95 (m, 4H, $H^{3,7,13,17}$), 8.49–8.47 (d, 2H, $H^{8,12}$, J = 7.85 Hz), 8.37–8.35 (d, 2H, $H^{2,18}$, J = 7.83 Hz), 8.23–8.21 (m, 2H, $H^{4\text{-HPh}}$), 8.12–8.09 (t, 1H, $H^{4\text{-HPh}}$, J = 7.14 Hz; J = 5.28 Hz), 8.05–8.03 (d, 2H, $H^{2,6\text{-HPh}}$, J = 8.1 Hz), 7.80–7.74 (m, 6H; 4H, $H^{3,5\text{-HPh}}$; 2H, $H^{2,6\text{-HPh}}$), 7.23–7.21 (m, 4H, $H^{2,6\text{-HPh}}$), 7.65–7.63 (m, 1H, benzothiazole), 7.62–7.59 (t, 1H, benzothiazole J = 7.72 Hz; J = 7.60 Hz), 7.57–7.55 (d, 1H, benzothiazole J = 7.57 Hz), 7.51–7.48 (t, 1H, benzothiazole J = 7.72 Hz; J = 7.59 Hz) 7.21–7.20 (m, 4H=3,5-Ph) ($CDCl_3$). UV-Vis (λ_{max}, (nm, logε): 596(3.75), 551(4.16), 424(5.52) ($CHCl_3$). MALDI-TOF MS: *m/z* calcd: $C_{51}H_{31}N_5SZn$, 811.2819; found: 811.6123.

Synthesis of zinc 5-[4'-(1",3"-benzoxazol-2"-yl)phenyl]-10,15,20-triphenylporphin (ZnPorO). In a 100-mL flask equipped with a magnetic stirrer and reflux condenser, a mixture of ZnPor (1 g, 0.132 mmol), $Pd(OAc)_2$ (0.0592 g, 0.264 mmol), $Cu(OAc)_2 \cdot H_2O$ (0.0575 g, 0.264 mmol), triphenylphosphine (0.34 g, 0.132 mmol), potassium carbonate (0.364 g, 1.342 mmol), and benzoxazole (0.314 g, 0.264 mmol) in toluene (45 mL) was refluxed with stirring for 52 h. Then the mixture was cooled to room temperature, dichloromethane (50 mL) was added, and the mixture was filtered. The precipitate was washed with dichloromethane (10 mL), and the organic fractions were combined and evaporated in vacuo. The residue was dissolved in dichloromethane (30 mL) and chromatographed on a silica gel column; elution was performed first with a hexane–dichloromethane mixture (1 : 1) to collect the tetraphenylporphin impurity band and then with dichloromethane to collect the dark red monoheterylporphyrin band. The solvent was evaporated to dryness. The yield was 0.131 g (64%). R_f 0.72 (Silufol, chloroform). ^{1}H NMR (δ, ppm): 9.00–8.95 (m, 4H, $H^{3,7,13,17}$), 8.67–8.66 (d, 2H, $H^{8,12}$, J = 7.67 Hz), 8.42–8.40 (d, 2H, $H^{2,18}$, J = 6.65 Hz), 8.24–8.23 (m, 2H, $H^{4\text{-HPh}}$), 8.12–8.11 (m, 1H, $H^{4\text{-HPh}}$), 7.96–7.94 (m, 2H, $H^{2,6\text{-HPh}}$), 7.94–7.92 (m, 6H, 4H, $H^{3,5\text{-HPh}}$; 2H, $H^{2,6\text{-HPh}}$), 7.79–7.73 (m, 4H, 2,6-HPh), 7.57–7.51 (m, 2H, benzoxazole), 7.48–7.46 (m, 2H, benzoxazole), 7.22–7.20 (d, 4H, $H^{3,5\text{-HPh}}$; J = 8.06 Hz) ($CDCl_3$). UV/Vis: λ_{max}, (nm, logε): 595(3.71), 552(4.10), 424(5.46) ($CHCl_3$). MALDI-TOF MS, *m/z:* calcd. for $C_{51}H_{31}N_5OZn$, 795.2154; found: 795.4511.

Synthesis of zinc 5-[4'-(*N*-methyl-1",3"-benzimidazol-2"-yl)phenyl]-10,15,20-triphenylporphin (ZnPorN). In a 100-mL flask equipped with a magnetic stirrer and reflux condenser, a mixture of ZnPor (1 g, 0.132 mmol), $Pd(OAc)_2$ (0.0592 g, 0.264 mmol), $Cu(OAc)_2$ (0.0575 g, 0.264 mmol), triphenylphosphine (0.34 g, 0.132 mmol), potassium carbonate (0.364 g, 1.342 mmol), and 1-methylbenzimidazole (0.349 g, 0.264 mmol) in toluene (45 mL) was refluxed with stirring for 52 h. Then the mixture was cooled to room temperature, dichloromethane (50 mL) was added, and the mixture was filtered. The precipitate was washed with dichloromethane (10 mL), and the combined organic fractions were evaporated in vacuo. The residue was dissolved in dichloromethane (30 mL) and chromatographed on a silica gel column; elution was performed first with a hexane–dichloromethane mixture (1 : 1) to collect the tetraphenylporphin impurity band and then with dichloromethane to collect the dark red monoheterylporphyrin band. The solvent was evaporated to dryness. The yield was 0.18 g (89%). R_f 0.55 (Silufol, chloroform). ^{1}H NMR (δ, ppm): 8.99–8.98 (m, 2H, $H^{8,12}$), 8.97–8.96 (m, 2H, $H^{2,18}$), 8.26–8.24 (m, 4H, $H^{3,7,13,17}$), 8.14–8.12 (m, 1H, $H^{4\text{-HPh}}$), 7.79–7.73 (m, 10H; 8H, $H^{2,6\text{-HPh}}$; 2H, $H^{4\text{-HPh}}$), 7.58–7.51 (m, 8H, $H^{3,5\text{-HPh}}$), 7.42–7.39 (m, 4H, N-methylbenzimidazole), 3.88 (s, 3H N–Me) ($CDCl_3$). UV-Vis: λ_{max}, (nm, logε): 595(3.70), 552(4.13), 424(5.50) ($CHCl_3$). MALDI-TOF MS, *m/z*: calcd. for $C_{52}H_{34}N_6Zn$, 808.2671; found: 808.6229.

RESULTS AND DISCUSSION

The unsymmetrical heteryl-substituted porphyrins ZnPorX (X = S, O, N) were synthesized starting from the unsymmetrical Por, which was obtained using mixed-aldehyde condensation of benzaldehyde and 4-bromobenzaldehyde (3 : 1 ratio) with pyrrole (Scheme 1). The reaction was carried out in a refluxing mixture of isomeric xylenes containing trifluoroacetic acid (1%) as a catalyst. The first step of the reaction (porphyrinogen formation) was carried out in an inert atmosphere, while the second one (porphyrinogen to porphyrin oxidation) was conducted in a flow of air oxygen. The resulting mixture of porphyrins was separated by column chromatography on alumina repeated two times. The bromo-substituted porphyrin was converted to ZnPor in a similar way [21]. Then the palladium-catalyzed coupling of bromo-substituted zinc(II) porphyrin with a heterocycle (benzothiazole,

benzoxazole, or N-methylbenzimidazole) was carried out by the procedures that we developed previously [22]. The $Pd(OAc)_2/Cu(OAc)_2$ (20/20 mol %) catalytic system was used in the presence of triphenylphosphine as a ligand and K_2CO_3 as a base. The catalytic heterylation reactions occurred within 30 h to give heterylporphyrins ZnPorX (X = S, O, N). It is noteworthy that despite the higher acidity of the C–H bond in the benzoxazole molecule and, hence, higher reactivity, ZnPorO is formed in the lowest yield (64%), unlike benzoxazole-substituted tripyridylporphyrin synthesized in our previous study [11]. The unsymmetrical heterylporphyrins ZnPorX were purified by column chromatography on silica gel, with the column being successively eluted with a hexane–dichloromethane (1 : 1) mixture and dichloromethane.

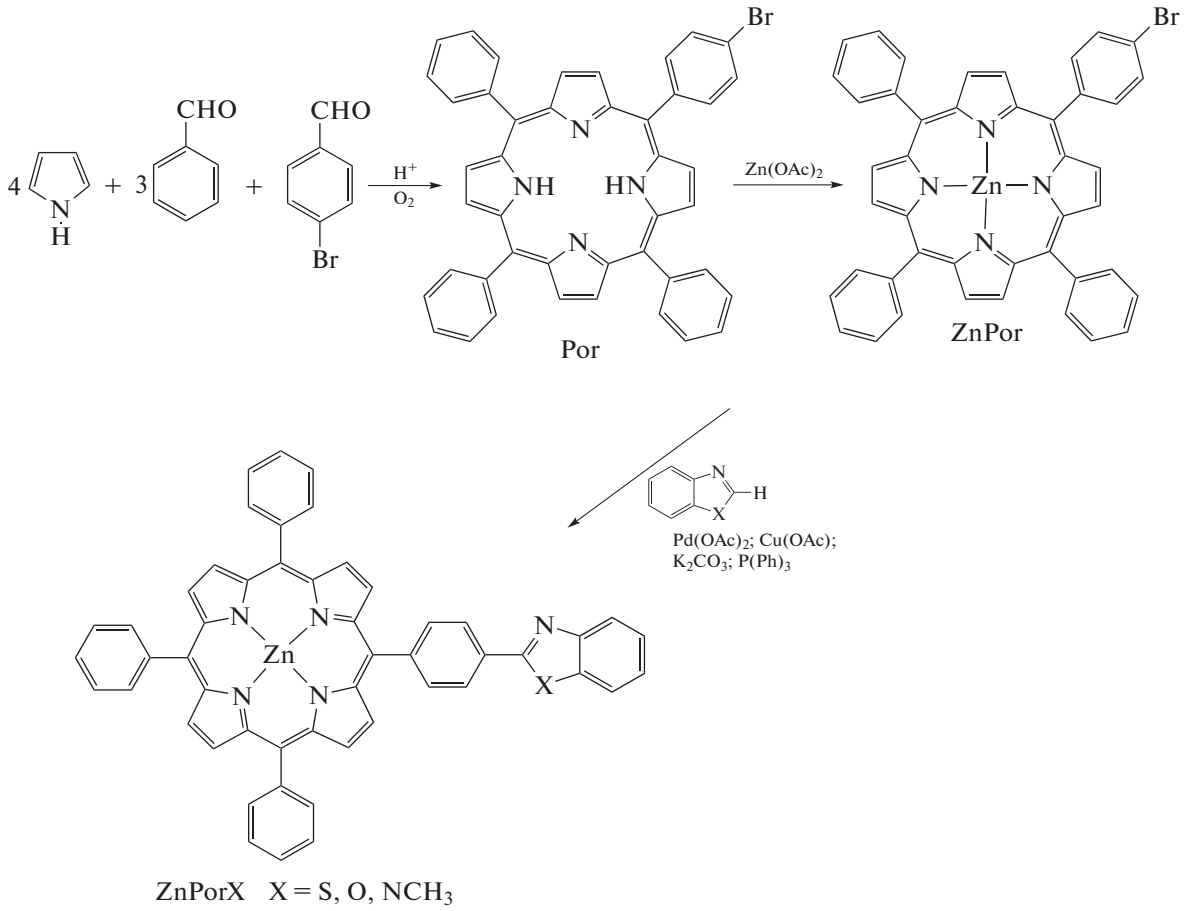

Scheme 1. Synthesis of unsymmetrical heteryl-substituted zinc(II) porphyrins.

The synthesized zinc(II) porphyrin complexes exhibit UV-Vis spectra typical of metal porphyrin complexes with D_{4h} symmetry of the macroheterocycle, which is manifested as intense absorption in the region of the Soret band (~425 nm) and two less intense bands in the visible region (~560 and 600 nm). As an example, Fig. 1a shows a typical UV-Vis spectrum of ZnPorO in DMF and in PBS–DMF (0.19 M). It is noteworthy that in aqueous media containing 0.19 M of DMF, the UV-Vis spectra of metal porphyrins are less resolved: the Soret band is broadened and red-shifted. The spectral changes observed on going from organic to aqueous organic medium attest to self-association of metal porphyrin molecules. A similar solvent effect is manifested in the fluorescence spectra of metal porphyrins (Fig. 1b). The metal porphyrin fluorescence is largely provided by the π-electron system of the macrocycle and is markedly affected by the fluorophore microenvironment. The π–π-interactions in the self-associates of zinc porphyrins lead to dissipation of the absorbed light energy and decreases the probability of fluorescence. The introduction of a heteryl substituent containing a benzothiazole, benzoxazole, or N-methylbenzimidazole residue into the zinc 5,10,15,20-tetraphenylporphyrin molecule increases the fluorescence quantum yield (Table 1). Apparently, the introduction of a bulky substituent into the *para*-position of the metal porphyrin benzene ring prevents the rotation of the peripheral substituent, thus partially stabilizing the state of the porphyrin macrocycle and reducing the probability of energy dissipation to vibrational pro-

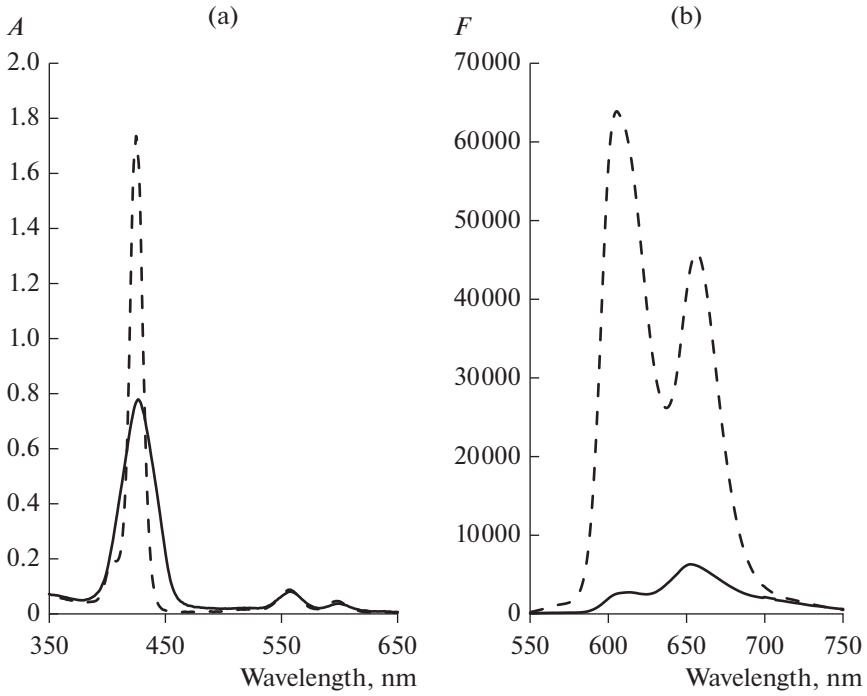

Fig. 1. (a) UV-Vis spectrum of ZnPorO (8.2×10^{-6} M) and (b) its fluorescence spectrum in DMF (dashed line) and in PBS–DMF (0.19 M) (continuous line).

cesses. The quantum yield of singlet oxygen, conversely, somewhat decreases upon the introduction of heteryl substituent into the zinc(II) tetraphenylporphyrin molecule (Table 1), but it still remains relatively high and allows one to consider the synthesized compounds to be potential photosensitizers for PDI.

As shown above, in the PBS–DMF medium (0.19 M), the synthesized porphyrins mainly exist in the associated state; they are stable against sedimentation in solution owing to the solvation with DMF. As solutions of zinc(II) porphyrins are titrated with albumin, the absorbance in the region of the Soret band in the UV-Vis spectra decreases. Whereas in the case of ZnPorS, this change does not exceed 1.5%, in the case of ZnPorO and ZnPorN, the decrease in the absorbance at 425 nm is 16 and 54%, respectively (Fig. 2). Furthermore, the absorbance at the Soret band in the UV-Vis spectrum of ZnPorN decreases by 43% upon the introduction of the first portion of albumin, while in the case of ZnPorO, the changes induced by titration are more steady. These results suggest that the following equilibria occur in the solutions:

$$(\mathrm{ZnPor})_n + \mathrm{DMF} \leftrightarrow m\mathrm{ZnPor} + (\mathrm{ZnPor})_{n-m}, \quad (1)$$

$$\mathrm{BSA} + \mathrm{DMF} \leftrightarrow \mathrm{BSA{\cdot}DMF}, \quad (2)$$

$$\mathrm{BSA} + \mathrm{ZnPor} \leftrightarrow \mathrm{BSA{\cdot}ZnPor}, \quad (3)$$

$$\mathrm{BSA} + (\mathrm{ZnPor})_{n-m} \leftrightarrow \mathrm{BSA{\cdot}}(\mathrm{ZnPor})_{n-m}. \quad (4)$$

Apparently, reactions (2) and (1) predominate in the case of ZnPorN and ZnPorO, and reactions (4) and (3) may take place for ZnPorO. In the case of ZnPorS, reactions (2) and (3) are relatively fast. To clarify the nature of intermolecular interactions, reverse fluorescence titration of BSA solutions with zinc(II) porphyrin solutions at the excitation wavelength of 295 nm was carried out. Under these conditions, the fluorescence of albumin is due to the presence of fluorophores, tryptophan residues, in the polypeptide chain. When ZnPorS is titrated with albumin, fluorescence quenching is observed (Fig. 3). This attests to the close proximity of the ZnPorS quencher to the tryptophan residues in the protein polypeptide chain, i.e., to the occurrence of reaction (3). The affinity constant of BSA to ZnPorS is relatively high, 6.05×10^5; unfortunately, albumin affinity to the other zinc(II) porphyrin cannot not be determined because

Table 1. Photochemical properties of metal porphyrins in aerated DMF at $\lambda_{excit} = 525$ nm

Complex	Φ_f^*, $\lambda_{excit} = 525$ nm	Φ_Δ^{**}, $\lambda_{excit} = 525$ nm
ZnPorS	0.09	0.52
ZnPorO	0.05	0.47
ZnPorN	0.04	0.54
ZnTPP [19]	0.03	0.7

* Φ_f is the fluorescence quantum yield.
** Φ_Δ is the quantum yield of singlet oxygen.

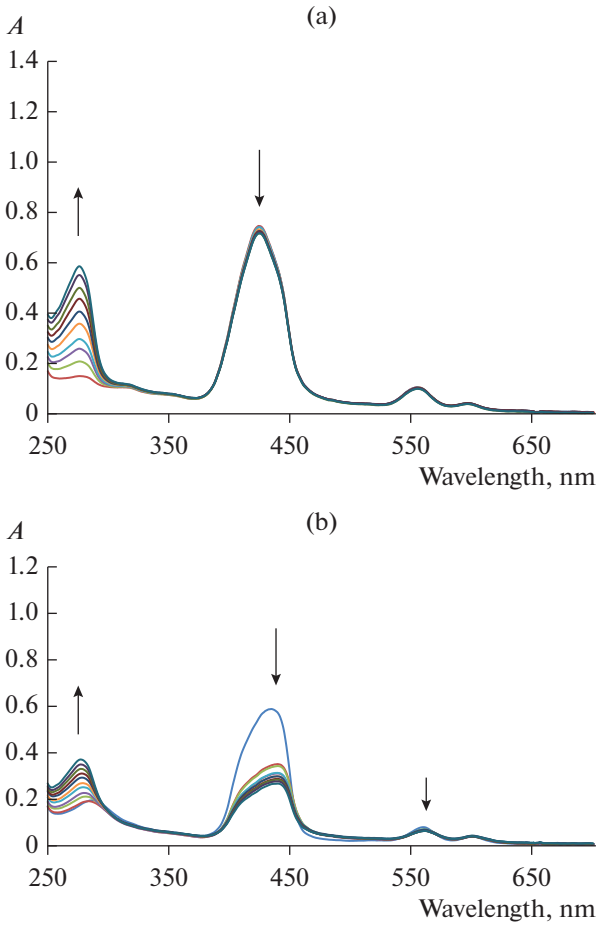

Fig. 2. (a) UV-Vis spectrum of ZnPorS (4.99×10^{-6} M) and (b) ZnPorN (6×10^{-6} M) in PBS–DMF (0.19 M) during titration with BSA ($0–6 \times 10^{-6}$ M).

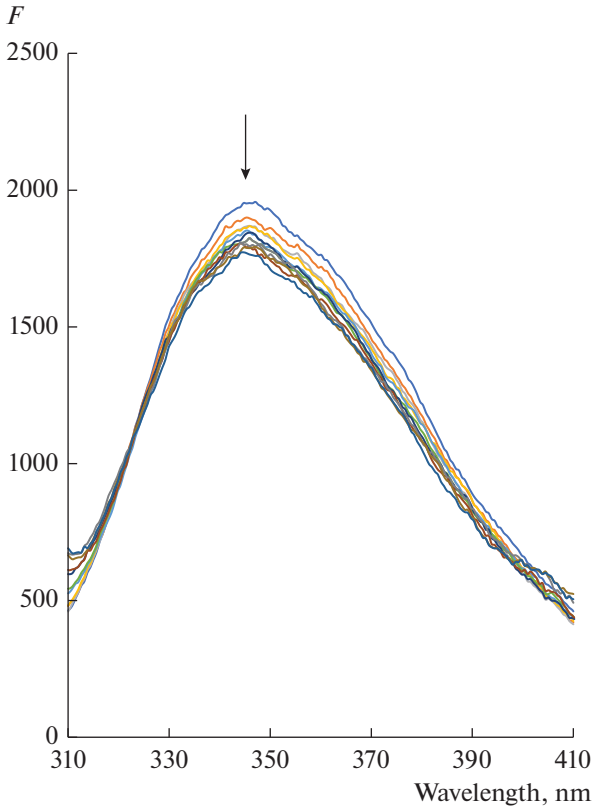

Fig. 3. Corrected fluorescence spectra of BSA (2.24×10^{-5} M) during titration with ZnPorS ($0–7.82 \times 10^{-6}$ M) in PBS–DMF (0.19 M) with allowance for the absorption of ZnPorS.

it is impossible to correctly take into account the internal filter effect for porphyrins ZnPorO and ZnPorN.

Since the fluorescence lifetime of a fluorophore is sensitive to its solvation/pseudo-solvation microenvironment, we studied the fluorescence quenching kinetics for zinc(II) porphyrins in DMF, PBS–DMF (0.3 M), and PBS–DMF–BSA (0.19 M). The fluorescence lifetime of analyzed zinc(II) porphyrins in DMF and in aqueous organic media is described by a biexponential dependence.

The experimental results for zinc(II) porphyrins in DMF and PBS–DMF were approximated by biexponential decay model:

$$I = A_1 e^{-\frac{t}{\tau_1}} + A_2 e^{-\frac{t}{\tau_2}}.$$

The average lifetime of the state was calculated by the formula:

$$\tau_{av} = \frac{A_1\tau_1^2 + A_2\tau_2^2}{A_1\tau_1 + A_2\tau_2},$$

where A_1 and A_2 are pre-exponential factors; τ_1 and τ_2 are lifetimes.

The resulting values are summarized in Table 2. The pre-exponential factors (A_i) reflect the proportion of fluorescent molecules with the fluorescence lifetime (τ_i). As can be seen from the data obtained in DMF and PBS–DMF, there are two components, one being short-lived ($\tau = 0.06–1.8$ ns). It is considered in the scientific literature that this short-lived state is due to dimerization/self-association of porphyrins [23] or to self-quenching effect caused by the Förster resonant energy transfer [24]. It is noteworthy that the fraction of the long-lived component ($\tau = 2–2.8$ ns) increases on going from an aqueous organic solvent to an organic solvent (Table 2). Probably, this fluorescence lifetime is inherent in monomeric zinc(II) porphyrins, mainly solvated by DMF molecules. The presence of albumin in the solutions changes the kinetics of zinc(II) porphyrin fluorescence: a longer-lived component ($\tau = 4.87–6.47$) appears in this case. It is worth noting that in the case of ZnPorO and ZnPorS in a BSA solution, the quenching kinetics is described by a tri-exponential dependence. The fluorophore exists in solution in at least three different states regarding the solvation envi-

Table 2. Fluorescence lifetime of zinc(II) porphyrins in solutions

Medium	τ_1, ns	A_1, %	τ_2, ns	A_2, %	τ_3, ns	A_3, %	τ_{aver}, ns	χ^2
ZnPorO								
PBS–DMF (0.3 M)	0.064	99.98	2.170	0.02			0.081	1.57
DMF	1.339	67.41	2.22	32.59			1.729	1.25
BSA–DMF (0.19 M)–PBS	0.149	90.86	1.112	7.53	4.87	1.62	1.665	1.42
ZnPorN								
PBS–DMF (0.3 M)	0.124	99.85	1.55	0.15			0.150	1.41
DMF	1.521	83.57	2.62	16.43			1.797	1.15
BSA–DMF (0.19 M)–PBS	1.756	93.27	6.47	6.73			2.75	1.32
ZnPorS								
PBS–DMF (0.3 M)	1.80	93.75	5	6.25				1.52
DMF	1.43	69.78	2.29	30.22			1.779	1.19
BSA–DMF (0.19 M)–PBS	0.20	90.42	1.05	8.64	5.46	0.95	1.282	1.41

ronment, which is in line with the participation of zinc(II) porphyrins in reactions ((1), (3), (4)).

An important part of the research is to evaluate the ability of porphyrins incorporated in biological structures to cause their irreversible changes. The observed rate constants of protein photooxidation in the presence of zinc(II) porphyrins and under photoirradiation at 425 nm were determined. Note that oxidation of the protein was detected only in systems where ZnPorS was used as a photosensitizer (Fig. 4). The other zinc(II) porphyrins do not exhibit a pronounced photocatalytic action.

Thus, the studies performed for a series of structural analogues of unsymmetrical zinc(II) porphyrins demonstrated that the photochemical properties of ZnPorS, the ability to photooxidize the alpha-helical protein, and the high affinity of the protein to the indicated porphyrin make it a promising candidate for being evaluated for the use in PDI.

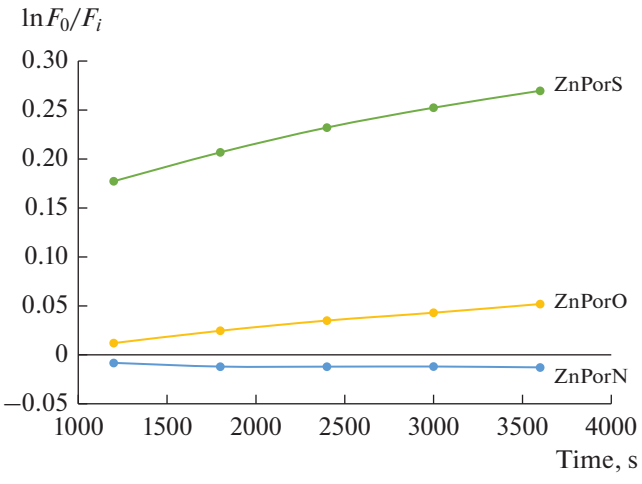

Fig. 4. Observed rate constants of the BSA photooxidation in the presence of ZnPorX under irradiation with light at 425 nm estimated as the ratio of BSA fluorescence before irradiation (lnF_0) to BSA fluorescence (F_i) under irradiation.

FUNDING

This study was supported by the Russian Science Foundation (grant no. 21-73-20140). Some of the research was carried out using the resources of the Upper Volga Regional Center for Physicochemical Research.

CONFLICT OF INTEREST

The authors of this work declare that they have no conflicts of interest.

REFERENCES

1. Mancuso, G., Midiri, A., Gerace, E., et al., *Pathogens*, 2021, vol. 10, p. 1310. https://doi.org/10.3390/*Pathogens*10101310
2. Urban-Chmiel, R., Marek, A., Stepie'n-Pysniak, D., et al., *Antibiotics*, 2022, vol. 11, no. 8, p. 1079. https://doi.org/10.3390/ANTIBIOTICS11081079
3. *Ten Threats to Global Health in 2019. World Health Organization*, 2019, vol. 22, p. 2021. https://www.who.int/news-room/spotlight/ten-threats-to-global-health-in-2019.
4. Kenawy, E.R., Worley, S.D., and Broughton, R., *Biomacromolecules*, 2007, vol. 8, no. 5, p. 1359. https://doi.org/10.1021/bm061150q
5. Stojiljkovic, I., Evavold, B.D., and Kumar, V., *Expert Opin. Invest. Drugs*, 2001, vol. 10, no. 2, p. 309. https://doi.org/10.1517/13543784.10.2.309
6. König, K., Teschke, M., Sigusch, B., et al., *Cell. Mol. Biol.*, 2000, vol. 46, no. 7, p. 1297.
7. Lebedeva, N.S., Gubarev, Y.A., Koifman, M.O., et al., *Molecules*, 2020, vol. 25, p. 4368. https://www.mdpi.com/1420-3049/25/19/4368.

8. Lebedeva, N.S. and Koifman, O.I., *Russ. J. Bioorg. Chem.*, 2022, vol. 48, no. 1, p. 1. https://doi.org/10.1134/S1068162022010071
9. Koifman, O.I., Ageeva, T.A., Beletskaya, I.P., et al., *Macroheterocycles*, 2020, vol. 13, no. 4, p. 183. https://doi.org/10.6060/mhc200814k
10. Koifman, O.I., Ageeva, T.A., Kuzmina, N.S., et al., *Macroheterocycles*, 2022, vol. 15, no. 4, p. 207. https://doi.org/10.6060/mhc224870k
11. Kiselev, A.N., Lebedev, M.A., Syrbu, S.A., et al., *Russ. Chem. Bull.*, vol. 71, no. 12, p. 2691. https://doi.org/10.1007/s11172-022-3698-5
12. Lebedeva, N.S., Yurina, E.S., Gubarev, Y.A., et al., *Mendeleev Commun.*, 2017, vol. 27, no. 1, p. 47. https://doi.org/10.1016/j.mencom.2017.01.014
13. Lebedeva, N.S., Yurina, E.S., Gubarev, Y.A., et al., *J. Inclus. Phenom. Macrocycl. Chem.*, 2019, vol. 95, nos. 3–4, p. 199. https://doi.org/10.1007/s10847-019-00947-1
14. Yurina, E.S., Gubarev, Y.A., Kiselev, A.N., et al., *Mendeleev Commun.*, 2020, vol. 30, no. 2, p. 211. https://doi.org/10.1016/j.mencom.2020.03.027
15. Lebedeva, N.S., Yurina, E.S., Gubarev, Y.A., et al., *Spectrochim. Acta, Part A*, 2021, vol. 246, p. 118975. https://doi.org/10.1016/j.saa.2020.11897.5
16. Lebedeva, N.S., Yurina, E.S., Gubarev, Y.A., et al., *Russ. J. Gen. Chem.*, 2019, vol. 89, p. 565. https://doi.org/10.1134/S1070363219030368
17. Ogunsipe, A. and Nyokong, T., *J. Mol. Struct.*, 2004, vol. 689, p. 89. https://doi.org/10.1016/j.molstruc.2003.10.024
18. Ormond, A.B. and Freeman, H.S., *Dyes Pigments*, 2013, vol. 96, no. 2, p. 440. https://doi.org/10.1016/j.dyepig.2012.09.011
19. Figueiredo, T.L.C., Johnstone, R.A., Sørensen, A.M.S., et al., *Photochem. Photobiol.*, 1999, vol. 69, no. 5, p. 517. https://doi.org/10.1111/j.1751-1097.1999.tb03322.x
20. Lebedeva, N.Sh., Mal'kova, E.A., Gubarev, Yu.A., et al., *Uch. Zap. Petrozavodsk. Gos. Univ.*, 2014, vol. 1, no. 8 (145), p. 12.
21. Rothemund, P. and Menotti, A.R., *J. Am. Chem. Soc.*, 1948, vol. 70, no. 5, p. 1808. https://doi.org/10.1021/ja01185a047
22. Kiselev, A.N., Syrbu, S.A., Lebedeva, N.Sh., et al., *Inorganics*, 2022, vol. 10, no. 63, p. 1. https://doi.org/10.3390/inorganics10050063
23. Akins, D.L., Özçelik, S., Zhu, H.R., et al., *J. Phys. Chem.*, 1996, vol. 100, no. 34, p. 14390. https://doi.org/10.1021/jp961013v
24. Ghosh, M., Nath, S., Hajra, A., et al., *J. Lumin.*, 2013, vol. 141, p. 87. https://doi.org/10.1016/j.jlumin.2013.03.025

Translated by Z. Svitanko